Templin, R. M., How, M., Roberts, N., Chiou, T-H., & Marshall, J. (2017). Circularly polarized light detection in stomatopod crustaceans: a comparison of photoreceptors and possible function in six species. *Journal of Experimental Biology*, *220*(18), [220]. https://doi.org/10.1242/jeb.162941

Circularly polarized light detection in stomatopod crustaceans: a comparision of photoreceptors and possible function in six species

Rachel M Templin[1], Martin J How[2], Nicholas W Roberts[2], Tsyr-Huei Chiou[3], Justin Marshall[1]

1- Queensland Brain Institute, University of Queensland, St Lucia, QLD 4072, Australia
2- School of Biological Sciences, University of Bristol, Bristol BS8 1TQ, UK
3- Department of Life Sciences, National Cheng Kung University, Tainan, Taiwan

Corresponding author: R Templin, email: r.templin@uq.edu.au

Keywords

Polarization vision, stomatopods, circular polarization, invertebrate vision

Summary statement

Based on the modelled birefringent properties of a photoreceptor cell (R8) many species of stomatopod achieve the optical function of quarter-wave retardance, allowing them to discriminate circularly polarized light.

Abstract

A combination of behavioural and electrophysiological experiments have previously shown that two species of stomatopod, *Odontadactylus scyllarus* and *Gonodactylaceus falcatus*, can differentiate between left and right handed circularly polarized light (CPL), and between CPL and linearly polarized light (LPL). It remains unknown if these visual abilities are common across all stomatopod species, and if so, how circular polarization sensitivity may vary between and within species. A sub-section of the midband, a specialized region of stomatopod eyes, contains distally placed photoreceptor cells, termed R8 (retinular cell number 8). These cells are specifically built with unidirectional microvilli and appear to be angled precisely to convert CPL into LPL. They are mostly quarter-wave retarders for human visible light (400-700nm) as well as being ultraviolet sensitive linear polarization detectors. The effectiveness of the R8 cells in this role is determined by their geometric and optical

properties. In particular, the length and birefringence of the R8 cells are critical for retardation efficiency. Here, our comparative studies show that most species investigated have the theoretical ability to convert CPL into LPL, such that the handedness of an incoming circular reflection or signal could be discriminated. One species, *Haptosquilla* trispinosa, shows less than quarter-wave retardance. While some species are known to produce circularly polarized reflections (some *Odontodactylus* species and *G. falcatus* for example), others do not, so a variety of functions for this ability are worth considering.

Introduction

Various aspects of vision are determined by environmental and behavioural need including overall sensitivity, spatial resolution, colour sensitivity and in some species, polarization sensitivity (PS). PS is common among invertebrates (Waterman and Horch, 1966; Schwind, 1991; Labhart and Meyer, 1999), but also found in vertebrates such as fish (Hawryshyn, 1992; Coughlin and Hawryshyn, 1995; Hawryshyn, 2003; Roberts et al., 2004; Roberts and Needham, 2007). As a source of visual information and as a visual cue, the polarization of light is used by many insects for navigation (Rossel, 1993; Labhart and Meyer, 2002; Dacke, 2003; Wehner and Muller, 2006) and water body location (Schwind, 1984; Horváth and Varju, 1997). Other invertebrates such as cephalopods and crustaceans also use polarization to increase visual contrast (Temple et al., 2012; How and Marshall, 2014; How et al., 2015) and for visual signalling (Cronin et al., 2009; Marshall et al., 2014).

Polarization is a fundamental property light and, in the context of animal vision, polarization refers to three measureable quantities for light that is made up of multiple waves (Goldstein, 2010). 1) The *angle of polarization* (AoP) defines the average angle at which the individual waves of light oscillate. If a linear polarizer is placed in the path of the light, then this is the angle at which the maximum intensity is transmitted. 2) *Ellipticity*: The electric fields of individual waves may be pictured as oscillating in a single plane or rotate as a circle or an ellipse around their direction of travel. Linearly polarized light (LPL) ocurs when the multiple waves within a beam of light waves oscillate, on average, in a single plane. This contrasts with circularly polarized light (CPL), where the rotating individual waves result, at any one point in time, in an equal measureable intensity in all directions. Elliptically polarized light (EPL) is the

most general form, in-between LPL and CPL. As a numerical value, *ellipticity* ranges from -1 or +1 for left-handed CPL to right-handed CPL respectively. A value in-between represents EPL and 0 is the special case for LPL.

Certain materials can change the ellipticity of polarized light according to their refractive index. The refractive index is an optical property relating to the speed that light is transmitted within a material. Some materials have more than one refractive index, which cause the components of a single wave of light to travel at different speeds. As one component lags behind the other, a phase difference is introduced. If this phase difference (or retardation) is equal to one quarter of the light's wavelength, individual waves can be imagined to rotate in a circle around the direction of propagation, either in a clockwise or anti-clockwise direction depending on the sign of the phase delay (Hecht, 1987, Goldstein, 2010). The retardation, δ, itself depends on both the birefringence (the difference between the refractive indices of a material), Δn, the wavelength, λ, and the thickness, t, of the material and is given by,

$$\delta(\lambda) = \frac{2\pi}{\lambda}\Delta n(\lambda)t. \quad (1)$$

An optical structure or device that creates a phase retardation of a quarter of a wavelength is called a quarter-wave retardation plate, or quarter-wave retarder. Materials that have the correct thickness and birefringence to convert LPL to CPL also work the opposite way, converting CPL to LPL. 3) The *degree of* or *percentage polarization* is the ratio of the (averaged) intensity of the polarized portion of the light to its total (averaged) intensity. For LPL, this is the extent to which multiple waves oscillate at the same angle of polarization. Man-made polarizing filters generally achieve a percentage polarization close to 100%. However, in nature, the percentage polarization of light is generally much lower. Light in the sky that scatters in the atmosphere has a maximum of around 60% (Wang et al., 2016) and can be around 40% in the ocean (Cronin et al., 2003a). Polarized animal signals can have a percentage polarizations of up to 80% (Marshall et al., 2014; Jordan et al., 2016).

Sensitivity to the polarization of light relies on the intrinsic PS of the retinal photoreceptors (Roberts at al., 2011). The rhabdomeric photoreceptors of invertebrates,

particularly insects and crustaceans, are polarization sensitive due to their orientational order and unidirectional microvilli (Snyder, 1973a; Snyder, 1973b; Roberts et al., 2011). Many crustaceans arrange their microvilli in two interdigitating perpendicular directions and position their photoreceptors relative to the outside world, allowing for maximal sensitivity to H and V polarized light (Waterman and Horch, 1966, Alkaladi et al., 2013, Marshall and Cronin, 2014). Stomatopods, benthic marine crustaceans, have a more complex retinal structure and organization of photoreceptors (Fig. 1A, B), which enables different information channels to be utilized in parallel (Marshall et al., 1991; Marshall and Cronin, 2014). The ommatidia in the dorsal and ventral hemispheres of stomatopod eyes follow similar organization seen in other crustaceans for sensitivity to linear polarization, except that the groups of microvilli in each hemisphere are oriented at $\pm 45^{\circ}$ with respect to each other (Marshall et al., 1991) (Fig. 1C). Furthermore, stomatopods exhibit a range of eye movements including rotation and scanning, and move their eyes both independently and asymmetrically. The ability to rotate their eyes around the eye-stalk axis makes the actual angle of PS relative to the world arbitrary, potentially allowing serial analysis of polarized light (Marshall et al., 1991) or specific optimization of PS for improving contrast of an object against a background (Daly et al., 2016).

Stomatopods use both LPL and CPL visual signals for inter- and intraspecific communication. Many species broadcast a variety of different linearly polarized visual signals (Cronin et al., 2003b; Cronin et al., 2003c; Chiou et al., 2005; Cronin et al., 2009a). For example, the first maxillipeds of many Haptosquillids are involved in sexual signals (Chiou et al., 2011) and recently, How *et al.* (2014) showed that the linearly polarized dimension of this signal had evolved through a mechanism of sensory bias. Circular polarization signalling may also facilitate communication (Chiou et al., 2008) and constitute a private communication channel for stomatopods, one which remains invisible to other animals, but highly salient to conspecifics (Gagnon et al., 2015). So far however, only a few species have been found with CPL reflections and there are some species that appear to lack any polarization signal at all, potentially relying only on colour. It is worth noting there are also several potential functions other than signalling such as contrast enhancement (Daly et al., 2016) or haze reduction (Schechner et al., 2003) that might make it worthwhile evolving sensitivity to one or both

types of polarized light. One of the purposes of the study described here was to begin to clarify which species have the potential sensory mechanism to detect CPL.

Stomatopod sensitivity to CPL relies on what are known as the R8 cells (retinular cell number 8) in the row 5 and 6 receptors of the midband photoreceptors (Fig. 1) (Chiou et al., 2008). The R8 cell occupies a position above the main R1-7 rhabdom and acts as a quarter-wave retarder, converting any incoming CPL to LPL. The result is that the underlying R1-7 rhabdoms become effectively sensitive to CPL by the fact that they detect the converted LPL. What is particularly unusual about the R8 cell is that the retardation is wavelength insensitive (achromatic). Whilst equation 1 describes how the retardation is an inverse function of wavelength, the effective birefringence of the R8 cell increases at longer wavelengths, cancelling out the effect of the change in wavelength and creating a constant retardation (Roberts et al., 2009). This wavelength-independent effective birefringence of the R8 cell occurs through a combination of the intrinsic birefringence of the microvillar membranes and a form birefringent component due to the ordered structure of sub-wavelength sized components (Born and Wolf, 1999). The effectiveness is therefore controlled by measureable characteristics of the cell; the length of the R8 rhabdom, the diameter of the microvillar tubes and the volume packing fraction of the microvilli in the cell (Fig. 2B, (Marshall et al., 1991)). Changes to either property alter the overall, effective birefringence of the cell.

The reliance on cell size for a specific retardance function is itself intriguing. When comparing different species of stomatopod, differences in body size exist: adult *Haptosquilla trispinosa* are usually less than 35mm in length compared to adult *Lysiosquillina maculata* which can grow to more than 30cm. Large size differences also exist developmentally within a species. For example the post-larvae of *L. maculata* are smaller by more than a factor of ten than the adults. There are concomitant differences in eye size and internal eye anatomy and changes to eye size could limit the space available to the R8 cell both optically and anatomically (Marshall et al., 1991). Any such changes may affect the retardance and optical function of the cell, unless one factor is adjusted relative to another, and investigating these changes was a second aim of this work. We also set out to quantify the potential differences in R8 cell size across different species of stomatopod and determine what effect body size has on the cells' function as a quarter-wave retarder. Attention was paid to differences that may

occur within species, such as differences between males and females, variation in size between individuals and finally any variation within eyes according to photoreceptor placement and packing.

Methods

Stomatopods were collected from coral reef and rubble, and mangrove areas around Lizard Island (14°40'40.8"S; 145°26'48.1"E) at a depth range of 0.5 to 5 m (GBRMPA Permit no. G12/35005.1, Fisheries Act no.140763). Species collected were *Gonodactylaceus falcatus*, *Gonodactylus smithii, Haptosquilla trispinosa* and *Lysiosquillina maculata*. Two further species, *Odontodactylus scyllarus* and *O. latirostris*, were collected from Shag Rock off North Stradbroke Island (27°25'0"S; 153°32'59.9"E) at a depth range of 10-20 m Moreton Bay Marine Park permit no: QS2013/CVL625). The animals represent species of a wide body length range (20-200 mm) in the Gonodactyloid and Lysiosquilloid superfamilies. Animals were either anesthetized and dissected at the field site, or transported live to the holding aquaria at the University of Queensland, St Lucia.

Retinal cell measurements

The animals were anesthetized by cooling on ice, decapitated, and both eyes were removed and fixed in 4% paraformaldehyde and 2.5% glutaraldehyde (in PEMS buffer) (adapted from (Chiou et al., 2005)). Samples were post fixed in 1% osmium tetroxide, and dehydrated in solutions with increasing ethanol concentrations. Samples were then infiltrated and embedded in EPON resin blocks for transmission electron microscopy (TEM). A microwave regime (Pelco Biowave, Ted Pella, USA) was used to aid dehydration (1 minute at 150 watts for each ethanol concentration) and infiltration (3 minutes at 150 watts under vaccum).

Embedded eyes were sectioned using an ultramicrotome (EM U26, Leica, Germany). Ultrathin (~60nm) and semithin (~500nm) coronal sections were obtained through the entire rhabdom in rows 5 and 6 of the midband (Fig. 2. Ultrathin sections were collected on copper grids and stained with 5% uranyl acetate in 50% ethanol and Reynolds Lead citrate for viewing in TEM (JEM- 1010, Jeol, Japan). Semithin sections were collected on glass slides and stained with toluidine blue for light microscopy (Bx61, Olympus, Japan).

Images of R8 cells were collected from the high acuity region of the eye (Marshall et al., 1991), along with other regions for comparison, using both TEM and light microscopy, which allowed for measurements to be made for both the length of the R8 cell and the width of the microvilli. Light microscopy was also used to make a separate set of measurements of the length for both the R8 and the R1-7 rhabdom. The total length of the rhabdom was obtained by adding the R8 and R1-7 measurements. Measurements were acquired from TEM images using iTEM imaging software (EMSIS, Muenster, Germany). To record the length of R8 cells across the whole eye, serial sections were obtained for light microscopy through the entire row 5 and 6. Images were registered in Fiji (Schindelin et al., 2012) and the positions of R8 cells digitized using custom Matlab-based scripts (Mathworks, 2016).

Model development and calculation of R8 retardation values

Using the methods developed by Roberts (2006) and Roberts et al. (2009), two-dimensional surface plots of retardation values were calculated based on R8 cell lengths and R8 microvilli diameter along with assumed refractive indices (Roberts et al., 2009). The surface plots allow direct visualization of the parameter sets that combine to create a specific retardation value. The contour lines depict particular values of retardance, with the bold line indicating the measurements required for quarter-wave functionality (0.25). All calculations were performed using R (v3.2.5, CRAN April 2016) and the script is available upon request. Effective dielectric tensors (Beche and Gaviot, 2003) were calculated for microvillar diameters in the range 20-85nm and photoreceptor lengths 40-120 microns. Onto these plots were mapped the experimentally measured values.

Statistical analysis

Data were analysed using a standardized major axis regression in R (v3.2.5, CRAN April 2016), using the smatr package, to determine the relationship between the entire rhabdom length and the length of the R1-7 and R8 rhabdoms across and between species.

Results

Total rhabdom measurements

Measurements of the R1-7 and R8 rhabdoms were completed using 16 individuals from 5 different species of stomatopod: (*Gonodactylus smithii* (n=5), *Odontodactylus scyllarus* (n=2), *Odontodactylus latirostris* (n=3), *Lysiosquillina maculata* (n=3) and *Haptosquilla trispinosa* (n=3) (Table 1 and Fig. 3). Measurement of the length of the R1-7 rhabdom and the R8 rhabdom were obtained from row 5 in all individuals and in row 6 for 13 individuals. An average total rhabdom length was calculated for each individual by averaging all measurements from rows 5 and 6. For each individual between 3 and 6 measurements were made for each row.

Conservation of R8 cell length

The rhabdom length varies between individuals based on body size (Fig. 3). Larger individuals have longer rhabdom lengths than smaller individuals. R1-7 cells account for the majority of the rhabdom and the length can vary greatly both within and between species. The R8 cell on the other hand is more consistent in length, with only small variability between individuals of differing body lengths (Fig. 3). Plotting the total rhabdom length against the length of the R1-7 cells shows a strong correlation between variables (R=0.99) which remains strong when considering individual species (Fig. 4A). The relationship between the total rhabdom and the R8 length is weaker (R = 0.54), indicating that the R8 cells are more constrained in length than the R1 -7 cells (Fig. 4B). Although the slopes for individual species do vary, the relationship between the R8 cell length and the total rhabdom length remains weak in all species.

R8 measurements for use in the calculation of the retardation

To further investigate the relationship between the length of the R8 rhabdom and the width of the individual microvilli within each R8 cell (Fig. 2, C and D) a second set of measurements were made from 25 individuals from 6 species of stomatopod; *Gonodactylus smithii* (n=7), *Gonodactylaceus falcatus* (n=3), *Odontodactylus scyllarus* (n=3), *Odontodactylus latirostris* (n=3), *Lysiosquillina maculata* (n=4) and *Haptosquilla trispinosa* (n=5) (Table 2). These measurements were obtained using only light microscopy preparations where the whole

length of the rhabdom could be measured. Measurements were acquired from 24 of the included individuals for row 5 and 22 for row 6. Measurements are only included here if they were obtained for both the length of the R8 and the width of the microvilli in a single row. The number of measurements made for each individual varied (from 2 to 15 measurements for R8 length, and 14 to 45 measurements for microvilli width) based on the alignment of the sections through the R8. The average R8 length and microvilli width were calculated for each individual (Table 2).

Variation between species

R8 cells vary slightly in their birefringent properties between species, although for most, this has little effect on their function as quarter-wave retarders. Figure 5 illustrates the birefringent properties of the R8 cells in each species. *O. scyllarus*, *O. latirostris*, *L. maculata*, *G. smithii* and *G. falcatus* (Fig. 5) all have R8 cells that fall close to the line which the model predicts will provide quarter-wave retardance, resulting in a circular polarization sensitivity in rows 5 and 6. In *H. trispinosa* the R8 cell measurements fall closer to the 0.2 line, suggesting that these cells convert CPL into EPL.

Variation within species

There was some variation in the size of the R8 cells, in relation to the length of the animal. This mostly affected species that displayed a large variation in body length, such as in *L. maculata* (which varied in body length from 32 mm to 200 mm) and in *O. scyllarus* (which varied from 45 mm to 167mm). The corresponding R8 cells varied from 64.03μm to 85.80μm in *L. maculata* and 41.87μm to 95.54μm in *O. scyllarus*, and resulted in variation in the cells calculated birefringence (Fig. 5). Essentially, small, presumably juvenile animals in these species possess R8 cells that would not convert circular polarization to linear but to EPL resulting in a weaker stimulation of the underlying R1-7 cells. In the case of the very small 45mm *O. scyllarus*, this would be around half that of a perfect quarter-wave retarder.

The smaller species, such as *G. falcatus*, *G. smithii*, *H. trispinosa* and *O. latirostris,* show less variation in R8 cell measurements, while also having less variation in body length, at least for the individuals we caught. It remains possible that very small just post-larval individuals in

these species might display similar birefringence variation. For *G. falcatus*, *G. smithii* and *O. latirostris* all the measurements within each species fall near the 0.25 line, indicating that they will be able to function as quarter-wave retarders. *H. trispinosa*, R8 cells fall close to the 0.2 line, suggesting either an elliptical sensitivity converting to LPL or just less efficient sensitivity to CPL as suggested for the smaller individuals of the larger species above.

Variation within the retina

The properties of the R8 can also vary across the length of the midband in a single eye. To investigate the variation within the eye measurements across the length of the midband were made in two speceis, *G. smithii* and *H. trispinosa*. The length of the R8 cells in row 5 and 6 in *G. smithii* varied across the eye, with the cells being significantly longer in the inner part of the eye compared to the outer part (Fig. 6A). Note however, the larger variation in R1-7 cells over this range. In *H. trispinosa* on the other hand, the R8 cell measurements remained a more constant size in the inner and outer part of the eye (Fig. 6B). When comparing these results to the birefringent model using the microvilli width coupled with the length of the R8s (Fig. 7) it appears that while the R8 cells in *H. trispinosa* function similarly across the whole midband, the R8 cells in *G. smithii* vary greatly in their ability to function as quarter-wave retarders across the midband. While the inner cells are longer than the optimal length, the outer cells are too short, and it is cells in and around the acute-zone that have R8 cells that fall within the correct size range for good quarter-wave retardance.

Discussion

The results of this study illustrate that, while there are several sources of variability in the size and thus the birefringence of the R8 cells across stomatopod species, R8s appear more conserved than other cells in the retina. This suggests adaptive pressure for R8 cells to stay within a certain size range to maintain the ability to act as quarter-wave retarders. There is a strong relationship between the length of the R1-7 cells and total rhabdom length, but less of a correlation between the R8 length and the total rhabdom length. This relationship highlights that the R8 length is conserved when the total size of the rhabdom increases.

Interspecies variability

Despite investigating several species of stomatopods with a large range of body sizes, habitat preferences and ecological constraints, the size of the R8 cells remained largely similar. As noted this suggests significant adaptive pressure to keep these cell types within a functional size range for quarter-wave retardance. The exception to this is *H. trispinosa* where the R8 cells retardance suggests sensitivity to an elliptical form of polarized light with retardance closer to 0.2 than 0.25. Why *H. trispinosa* would be tuned to detect elliptical polarized light (EPL) is yet known, but it is fascinating to speculate that its eye may be tuned more specifically to a particular ellipticity in the environment. Alternatively, selection for precise quarter-wave retardance in this species may be relaxed, as CPL is less significant for its current survival needs. Notably, this species does display strong linear polarization signals (Cronin et al., 2009a).

Body size

Within a species, most cells perform well as quarter-wave retarders, but there was some individual variability, particularly where the total body size of the animals varied greatly from juvenile to adult, such as *L. maculata* and *O. scyllarus*. This indicates that, while large individuals of a species detect circularly polarized light, small individuals of the same species, perhaps not yet sexually mature and with no need to pay attention to circular polarization, may not. In these cases, instead of opting for a shorter R1-7 rhabdom, the birefringent function of the R8 cell is compromised, suggesting a critical R1-7 length is required for the rhabdom to maintain sensitivity. Additionally, once the R8 has reached the point of quarter-wave retardance it no longer continues to increase in size. That is the R8 seems to stop increasing in size at sensitivity to circularly polarized light, allowing large relative increases in the R1-7 rhabdom.

Sensitivity changes within the eye

Investigation of R8 sizes across the midband in *H. trispinosa* and *G. smithii* provided evidence that R8 cell length can also vary within an individual eye. While the length of the R8s in *H. trispinosa* displayed a similar size across the midband*, G. smithii* displays more variability in R8 cell length, with the inner, more forward facing, part of the midband having longer R8 cells than the outer, lateral part. In fact *G. smithii* only have circular polarization sensitivity in the

central part of the midband, in ommatidia around the acute zone. It may be that the elongate design of this eye places spatial limits on the ommatidial dimensions and that retaining good CPL sensitivity in the forward-facing zones is enough. The eye of *H. trispinosa* is evenly spherical along the mid-band direction (as are the eyes of all other species examined (Marshall et al 1991a; Marshall and Land 1993)) making it possible to retain the same R8 dimensions along the whole midband, including the acute zone, without compromising the size of the R1-7.

Function of circular polarization vision

Previous behavioural tests have shown *O. scyllarus* can learn left from right circular polarization in feeding trials (Chiou et al., 2008). It is also known that *G. falcatus* prefers not to enter burrows emitting circularly polarized light (Gagnon et al., 2015), however the actual use of CPL in either of these species or others included in this study is still hypothetical. It is not known, for instance, if food items of *O. scyllarus* reflect CPL differentially, or if this species just manages to transfer its ability for discrimination to an isolated feeding circumstance in behavioural trials. *Odontodactylus* species and specifically *G. falcatus* are known to reflect CPL (Chiou et al 2008; Gagnon et al 2015) and one possible function is inter or intra-specific signalling. However this is yet to be directly tested. In the context of other animals, scarab beetles have been known for many years to reflect CPL (Michelson, 1911) and initial behaviour evidence suggested sensitivity to CPL in American jewel beetles (Brady and Cummings, 2010). However, this sensitivity was not found in a more recently conducted survey of four related European species (Blaho et al., 2012). If CP is used by stomatopods for inter or intra-specific signalling, it should be noted that so far only *Odontodactylus cultrifer*, *G. falcatus, Squilla mantis* and some *Neogonodactylus* species are known to exhibit strongly polarized CP reflections (Chiou et al., 2008; Gagnon et al., 2015), but further investigation is underway to quantify polarized signals more thoroughly in other species.

LPL insensitive detection channels

Finally, it is worth considering that the R8 cells in rows 5 and 6 of the midband may not have originally evolved with the primary purpose of converting CPL to LPL. The R8 cells in rows 5 and 6 are sensitive to ultraviolet wavelengths of light because the R8 of row 5 is orientated perpendicular to the R8 of row 6, and by comparison they act as an ultraviolet PS channel

(Kleinlogel and Marshall, 2009) in the midband sensitive to LPL. However, if the R1-7 photoreceptors below are primarily concerned with colour vision or a measure of intensity (Marshall et al., 1991; Theon et al., 2014), then elimination of PS is ideal and allowing them to potentially be subject to false colours (Kelber et al., 2001) or false signals. Other arthropods avoid sensitivity to LPL by 1) producing rhabdomeres with microvilli that are misaligned, 2) forming twisted rhabdomeres with microvilli of low birefringence, or 3) the signals of receptors with mutually perpendicular microvilli are summed in the lamina (Eguchi and Waterman, 1968; Eguchi and Waterman, 1973; Waterman, 1981; Marshall et al., 1991). The use of the R8 cell as a quarter-wave retarder provides a novel approach to remove the linear polarization information in the signal. Interestingly, this way of removing unwanted LPL is also used in photography, where CPL rather than LPL filters are used (Goldberg, 1992). A clear, although again hypothetical, evolutionary progression could therefore drive a quarter-wave retarder to be exploited through the emergence of CPL signals to provide certain species with the sensory ability to detect CPL.

While several alternative, and not necessarily mutually exclusive, hypotheses exist for the evolution of this apparently complex polarization vision system, it is worth re-iterating that our knowledge of what the stomatopods actually do with polarization vision and polarized reflections, where they exist, is still in its infancy. What is required are field observations and behavioural analyses that would help place such hypotheses on a firm foundation of reality.

Abbreviation list

CLP - circularly polarized light

EPL - elliptically polarized light

LPL - linearly polarized light

CP - circular polarization

PS - polarization sensitivity

R8 - eighth retinular cell

Acknowledgements

The authors wish to acknowledge the facilities, and the scientific and technical assistance, of the Australian Microscopy and Microananalysis Research Facility at the Centre for

Microscopy and Microanalysis, The University of Queensland. And Dr Hanne Thoen for her comments on the manuscript.

Funding

This work was supported by grants awarded to JM Asian Office of Aerospace Research and Development (AOARD- 12-4063) and the Australian Research Council (FL140100197), and to NWR Air Force Office of Scientific Research (AFOSR FA8655-12-2112).

Competing interests

No competing interests declared

Contributions

RMT, MJH, NWR, TC and JM designed the study. RMT and MJH collected and analysed the microscopy data, NWR wrote the mathematical models for the retardation calculation and RMT produced the modeled data. RMT, MJH, NWR, TC and JM contributed to writing and editing the manuscript.

References

Alkaladi, A., How, M. J. & Zeil, J. 2013. Systematic variations in microvilli banding patterns along fiddler crab rhabdoms. *J Comp Physiol A Neuroethol Sens Neural Behav Physiol,* 199**,** 99-113.

Beche, B. & Gaviot, E. 2003. Matrix formalism to enhance the concept of effective dielectric constant. *Optics Communication,* 219**,** 15-19.

Blaho, M., Egri, A., Hegedus, R., Josvai, J., Toth, M., Kertesz, K., Biro, L. P., Kriska, G. & Horvath, G. 2012. No evidence for behavioral responses to circularly polarized light in four scarab beetle species with circularly polarizing exocuticle. *Physiol Behav,* 105**,** 1067-75.

Born, M. & Wolf, E. 1999. *The principles of optics,* Cambridge, Cambridge University Press.

Brady, P. & Cummings, M. 2010. Differential response to circularly polarized light by the jewel scarab beetle Chrysina gloriosa. *Am Nat,* 175**,** 614-20.

Chiou, T.-H., Cronin, T. W., Caldwell, R. L. & Marshall, J. 2005. Biological polarized light reflectors in stomatopod crustaceans. 5888**,** 58881B-58881B-9.

Chiou, T.-H., Marshall, N. J., Caldwell, R. L. & Cronin, T. W. 2011. Changes in light-reflecting properties of signalling appendages alter mate choice behaviour in a stomatopod crustacean Haptosquilla trispinosa. *Marine and Freshwater Behaviour and Physiology,* 44**,** 1-11.

Chiou, T. H., Kleinlogel, S., Cronin, T., Caldwell, R., Loeffler, B., Siddiqi, A., Goldizen, A. & Marshall, J. 2008. Circular polarization vision in a stomatopod crustacean. *Curr Biol,* 18**,** 429-34.

Coughlin, D. J. & Hawryshyn, C. W. 1995. A cellular basis for polarized-light vision in rainbow trout. *J Comp Physiol A,* 176**,** 261-272.

Cronin, T. W., Chiou, T.-H., Caldwell, R. L., Roberts, N. & Marshall, J. Polarization signals in mantis shrimps. Proc. SPIE, 2009a. 74610C-74610C-10.

Cronin, T. W., Shashar, N., Caldwell, R. L., Marshall, J., Cheroske, A. G. & Chiou, T. H. 2003a. Polarization signals in the marine environment. *In:* SHAW, J. A. & TYO, J. S. (eds.) *Polarization Science and Remote Sensing.* Bellingham: Spie-Int Soc Optical Engineering.

Cronin, T. W., Shashar, N., Caldwell, R. L., Marshall, J., Cheroske, A. G. & Chiou, T. H. 2003b. Polarization vision and its role in biological signalling. *Integrative and Comparative Biology,* 43**,** 549-558.

Cronin, T. W., Shashar, N., Caldwell, R. L., Marshall, J. N., Cheroske, A. G. & Chiou, T. H. 2003c. Polarization signals in the marine environment. *Proceedings of SPIE,* 5158**,** 85-92.

Dacke, M. 2003. Twilight orientation to polarised light in the crepuscular dung beetle Scarabaeus zambesianus. *Journal of Experimental Biology,* 206**,** 1535-1543.

Daly, I. M., How, M. J., Partridge, J. C., Temple, S. E., Marshall, N. J., Cronin, T. W. & Roberts, N. W. 2016. Dynamic polarization vision in mantis shrimps. *Nat Commun,* 7**,** 12140.

Eguchi, E. & Waterman, T. H. 1968. Cellular basis for polarized light perception in the spider crab, *Libinia*. *Zeitschrift für Zellforschung und Mikroskopische Anatomie,* 84**,** 87-101.

Eguchi, E. & Waterman, T. H. 1973. Orthogonal microvillus pattern in the eigth rhabdomere of the rock crab Grapsus. *Z.Zellforsch,* 137**,** 145-157.

Gagnon, Y. L., Templin, R. M., How, M. J. & Marshall, N. J. 2015. Circularly Polarized Light as a Communication Signal in Mantis Shrimps. *Curr Biol,* 25**,** 3074-8.

Goldberg, N. 1992. *Camera technology: The dark side of the lens,* Cambridge, United States of America, Academic Press.

Goldstein, D. 2010. Introduction to Polarized Light. *Polarized Light, Third Edition.* CRC Press.

Hawryshyn, C. W. 1992. Polarisation vision in fish. *American Scientist,* 80**,** 164-175.

Hawryshyn, C. W. 2003. Mechanisms of Ultraviolet Polarization Vision in Fishes. *In:* COLLIN, S. P. & MARSHALL, N. J. (eds.) *Sensory Processing in Aquatic Environments.* Springer New York.

Hecht, E. 1987. *Optics*, Addison Wesley.

Horváth, G. & Varju, D. 1997. Polarization patter of freshwater habitats recorded by video polarimetry in red, green and blue spectral anges and its relevance for water detection by aquatic insects. *J Exp Biol,* 200**,** 1155-1163.

How, M. J., Christy, J. H., Temple, S. E., Hemmi, J. M., Marshall, N. J. & Roberts, N. W. 2015. Target Detection Is Enhanced by Polarization Vision in a Fiddler Crab. *Curr Biol,* 25**,** 3069-73.

How, M. J. & Marshall, N. J. 2014. Polarization distance: a framework for modelling object detection by polarization vision systems. *Proc Biol Sci,* 281**,** 20131632.

Jordan, T. M., Wilby, D., Chiou, T. H., Feller, K. D., Caldwell, R. L., Cronin, T. W. & Roberts, N. W. 2016. A shape-anisotropic reflective polarizer in a stomatopod crustacean. *Sci Rep,* 6**,** 21744.

Kelber, A., Thunell, C. & Arikawa, K. 2001. Polarisation-dependant colour vision in *Papilio* butterlies. *J Exp Biol,* 204**,** 2469-2480.

Kleinlogel, S. & Marshall, N. J. 2009. Ultraviolet polarisation sensitivity in the stomatopod crustacean Odontodactylus scyllarus. *J Comp Physiol A Neuroethol Sens Neural Behav Physiol,* 195**,** 1153-62.

Labhart, T. & Meyer, E. P. 1999. Detectors for polarized skylight in insects: a survey of ommatidial specializations in the dorsal rim area of the compound eye. *Microscopy Research and Technique,* 47**,** 368-379.

Labhart, T. & Meyer, E. P. 2002. Neural mechanisms in insect navigation: polarization compass and odometer. *Curr Opin Neurobiol,* 12**,** 707-714.

Marshall, J., Land, M. F., King, C. A. & Cronin, T. W. 1991. The compound eyes of mantis shrimps (Crustacea, Hoplocarida, Stomatopoda). I. Compound eye structure: The detection of polarized light. *Philos Trans R Soc Lond B Biol Sci,* 334**,** 33-56.

Marshall, J. N. & Cronin, T. W. 2014. Crustacean Polarization vision. *Polarized light and polarization vision in animal sciences.* New York: Springer.

Marshall, N. J., Roberts, N. W. & Cronin, T. W. 2014. Polarization signals. *Polarized light and polarization vision in animal science.* Springer.

Michelson, A. A. 1911. LXI. On metallic colouring in birds and insects. *Philosophical Magazine Series 6,* 21**,** 554-567.

Roberts, N. W. 2006. The optics of vertebrate photoreceptors: anisotropy and form birefringence. *Vision Res,* 46**,** 3259-66.

Roberts, N. W., Chiou, T. H., Marshall, J. & Cronin, T. W. 2009. A biological quater-wave retarder with excellent achromaticity in the visible wavelength region. *Nature Photonics,* 3**,** 641-644.

Roberts, N. W. & Needham, M. G. 2007. A mechanism of polarized light sensitivity in cone photoreceptors of the goldfish Carassius auratus. *Biophys J,* 93**,** 3241-8.

Roberts, N. W., Porter, M. L. & Cronin, T. W. 2011. The molecular basis of mechanisms underlying polarization vision. *Philos Trans R Soc Lond B Biol Sci,* 366**,** 627-37.

Roberts, N. W., Temple, S. E., Haimberger, T. J. & Hawryshyn, C. W. 2004. Differences in the optical properties of vertebrate photoreceptor classes leading to axial polarization sensitivity. *J. Opt. Soc. Am. A,* 21**,** 355-345.

Rossel, S. 1993. Navigation by bees using polarised skylight. *Comparative Biolchemistry and Physiology,* 104A**,** 965-708.

Schechner, Y. Y., Narasimhan, S. G. & Nayar, S. K. 2003. Polarization-based vision Through Haze. *Applied Optics,* 42, 511-525.

Schindelin, J., Arganda-Carreras, I., Frise, E., Kaynig, V., Longair, M., Pietzsch, T., Preibisch, S., Rueden, C., Saalfeld, S., Schmid, B., Tinevez, J. Y., White, D. J., Hartenstein, V., Eliceiri, K., Tomancak, P. & Cardona, A. 2012. Fiji: an open-source platform for biological-image analysis. *Nat Methods,* 9**,** 676-82.

Schwind, R. 1984. Evidence for true polarization vision based on a two-channel analyzer system in the eye of the water bug, Notonecta glauca. *J Comp Physiol A,* 154**,** 53-57.

Schwind, R. 1991. Polarization vision in water insects and insects living on a moist substrate. *J Comp Physiol A* 169**,** 531-540.

Snyder, A. W. 1973a. Polarization sensitivity of individual retinula cells. *Journal Comparative Physiology A,* 83**,** 331-360.

Snyder, A. W. 1973b. Structure and function of the fused rhabdom. *J Comp Physiol A,* 87**,** 99-135.

Temple, S. E., Pignatelli, V., Cook, T., How, M. J., Chiou, T. H., Roberts, N. W. & Marshall, N. J. 2012. High-resolution polarisation vision in a cuttlefish. *Curr Biol,* 22**,** R121-2.

Wang, X., Gao, J., Fan, Z. & Roberts, N. W. 2016. An analytical model for the celestial distribution of polarized light, accounting for polarization singularities, wavelength and atmospheric turbidity. *Journal of Optics,* 18**,** 065601.

Waterman, T. H. 1981. *Polarisation sensitivity In: Autrum H (ed) Handbook of Sensory physiology, vol VII/6B,* Berlin, Heidelberg, New York, Springer-Verlag.

Waterman, T. H. & Horch, K. W. 1966. Mechanisms of polarized light perception. *Science,* 154**,** 467-475.

Wehner, R. & Muller, M. 2006. The significance of direct sunlight and polarized skylight in the ant's celestial system of navigation. *Proc Natl Acad Sci U S A,* 103**,** 12575-9.

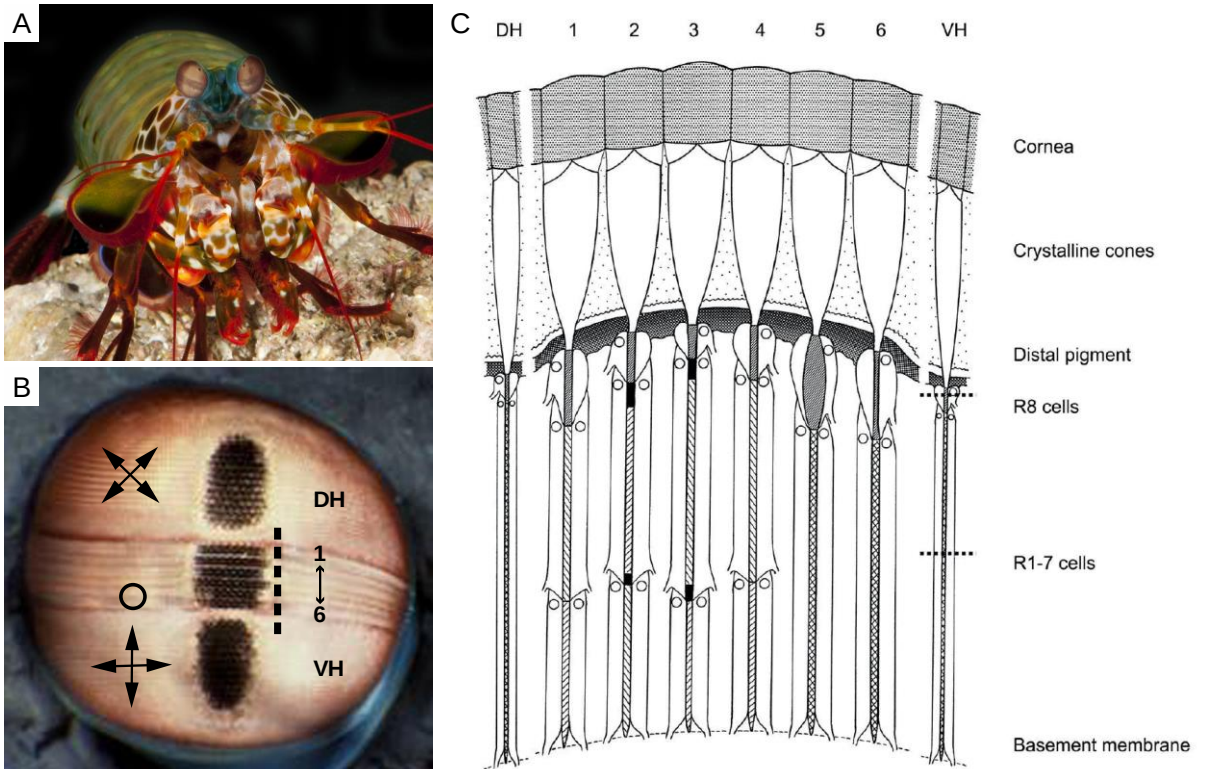

Figure 1: Eye structure of stomatopod crustaceans. *Odontodactylus scyllarus* (A) and eye (B) showing the pseudo pupils of the three sections, the dorsal (DH) and ventral (VH)

hemispheres and the midband (showing midband rows 1 to 6). A and B photos: Roy Caldwell. The microvillar direction and resultant linear polarization of the hemispheres are represented by the crossed arrows, the circular polarization sensitivity in rows 5 and 6 by the circle. The dashed line shows the area of the retina depicted in the diagrammatic section in (C) (Marshall et al., 1991)

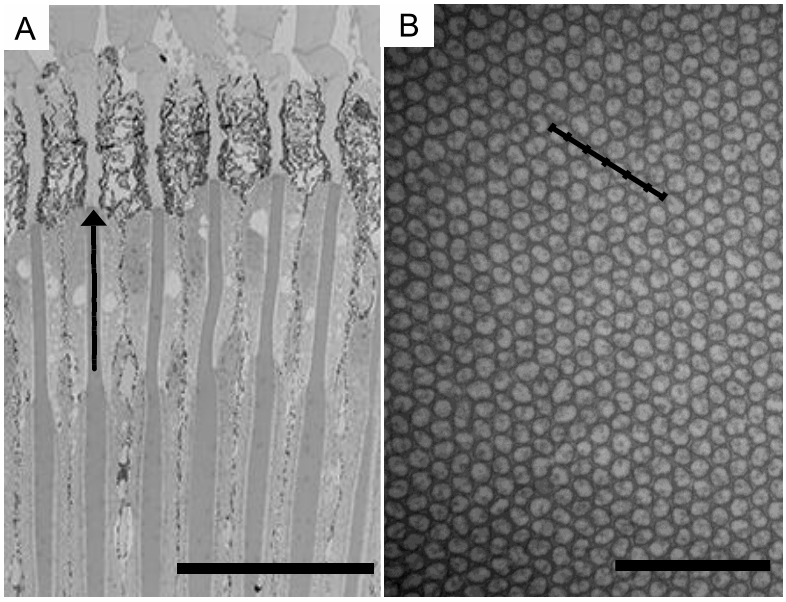

Figure 2: R8 cell anatomy A) 90° cross section through the R8 cells of midband row 5, arrow indicates the length of the R8 cell. B) 90° cross section through the tightly packed unidirectional microvilli of a Row 6 R8 cell. Scale bars: A) 100μm B) 400nm.

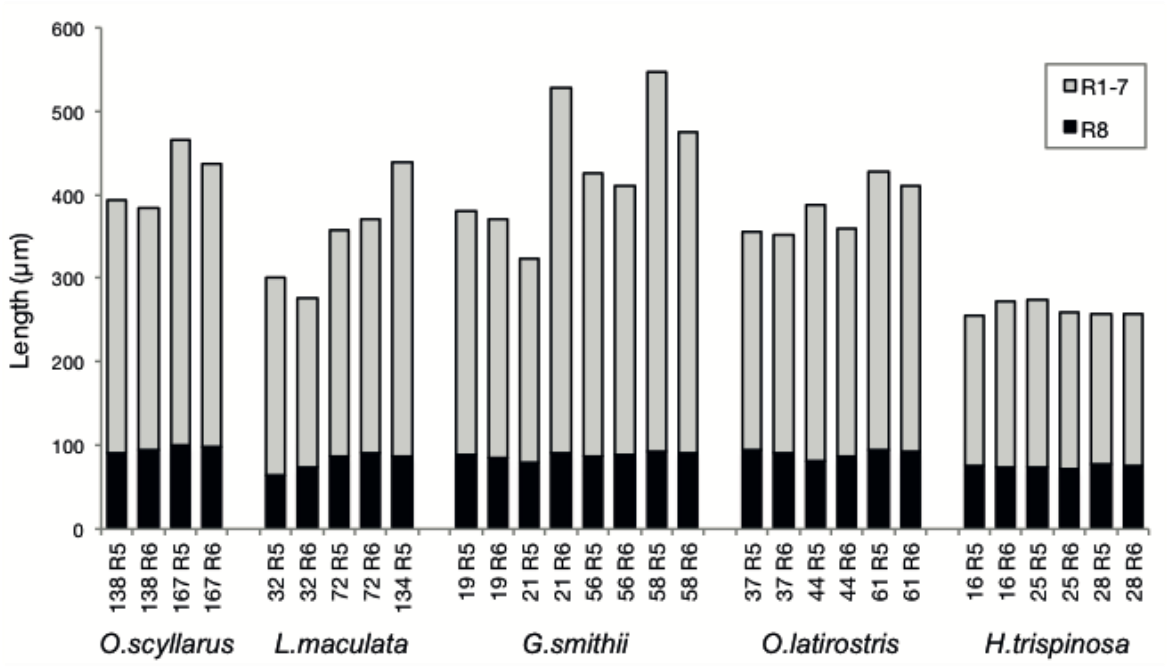

Figure 3: Total rhabdom lengths from 5 species of stomatopod. The bars show the average total length of the rhabdoms of row 5 and 6 of the acute zone of individuals from 5 species of stomatopod, *O. scyllarus* (n=2), *L. maculata* (n=3), *G. smithii* (n=4), *O. latirostris* (n=3), and *H. trispinosa* (n=3). Each bar is divided into R8 (black) and R1-7 (grey). Bar labels show the individual body length (mm) and midband row, row 5 (R5) or 6 (R6).

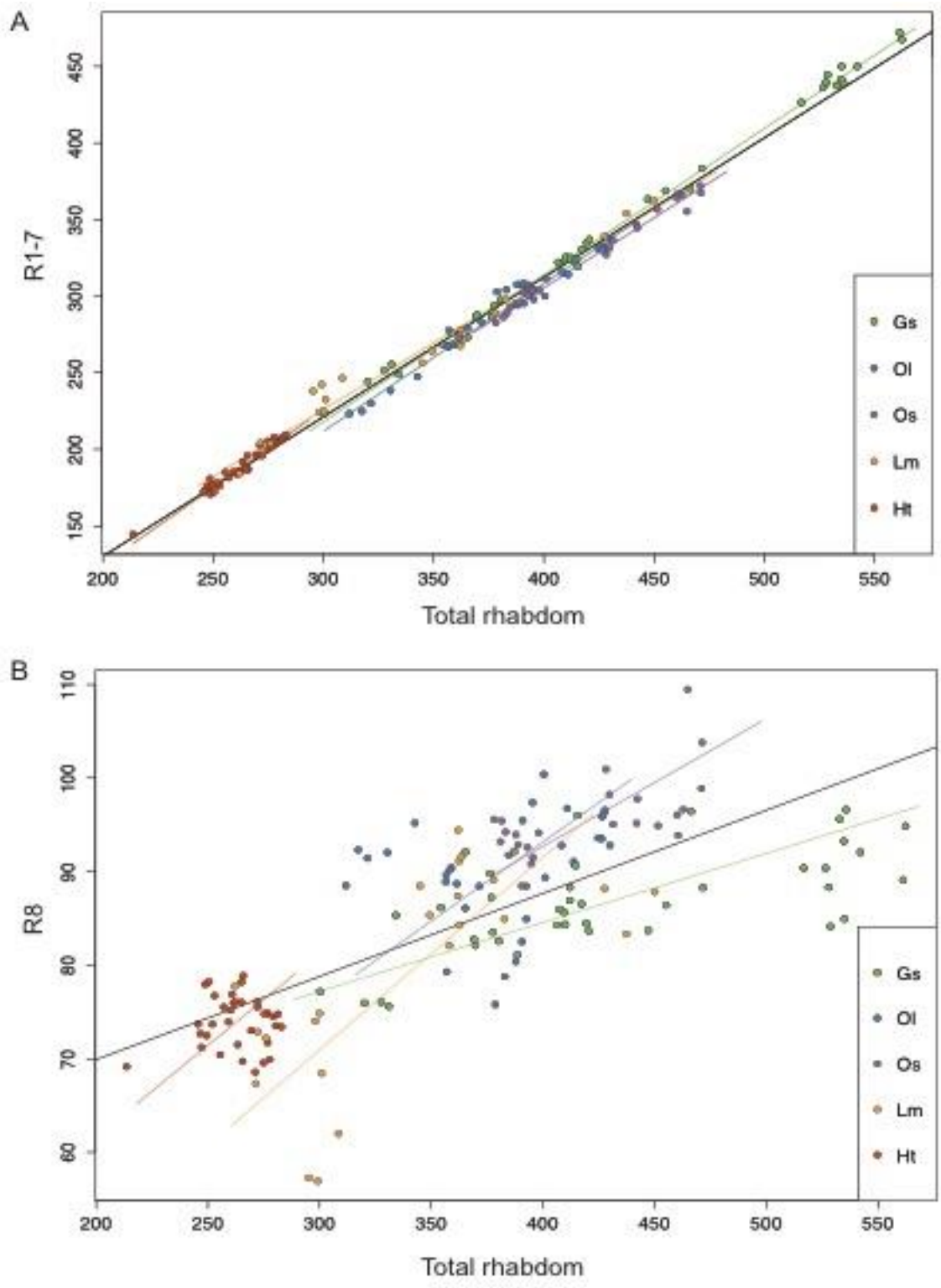

Figure 4: Relationship of R1-7 and R8 to the total rhabdom length. A and B include measurements for both rows 5 and 6 from 5 species of stomatopod, *G. smithii* (Gs, n=4), *O. latirostris* (Ol, n=3), *O. scyllarus* (Os, n=2), *L. maculata* (Lm, n=3) and *H. trispinosa* (Ht, n=3). Each graph shows the slope for the overall data set (back) and one for each species. A) relationship of R1-7 length and total rhabdom length (Overall R= 0.99, Gs R=0.99, Ol R=0.97,

Os R= 0.99, Lm R=0.97, Ht R=0.96). B) Relationship of R8 length to total rhabdom length (Overall R= 0.54, Gs R=0.41, Ol R=0.8, Os R=0.42, Lm R=0.48, Ht R=0.002).

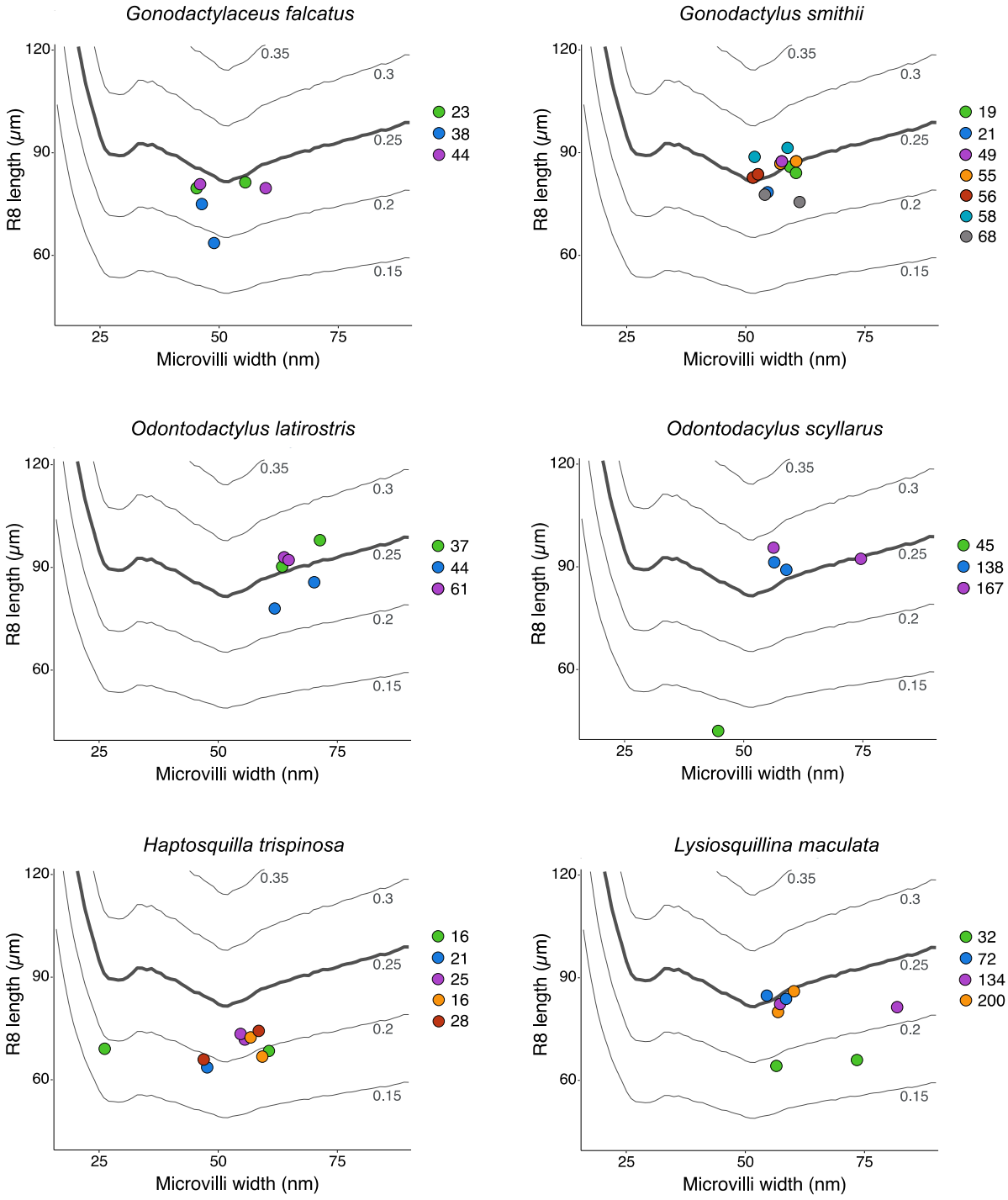

Figure 5: Birefringent properties of R8 cells from different species of stomatopod. This figure combines the measurements for the R8 cells with the calculations of retardation values to predict the birefringence in different species *G. falcatus* (n=3), *G. smithii* (n=7), *O. latirostris* (n=3), *O. scyllarus* (n=3), *H. trispinosa* (n=5) and *L. maculata* (n=4). Contour lines represent

modelled retardance value for corresponding R8 cell length and microvillus widths. Bold contour lines represent the value for quarter-wave retardance (0.25). Each point is the average of measurements (R8 length and microvillus length) for either row 5 or row 6 with different individuals shown in different colours and their body lenth (in mm) is listed in the associated legend for each panel.

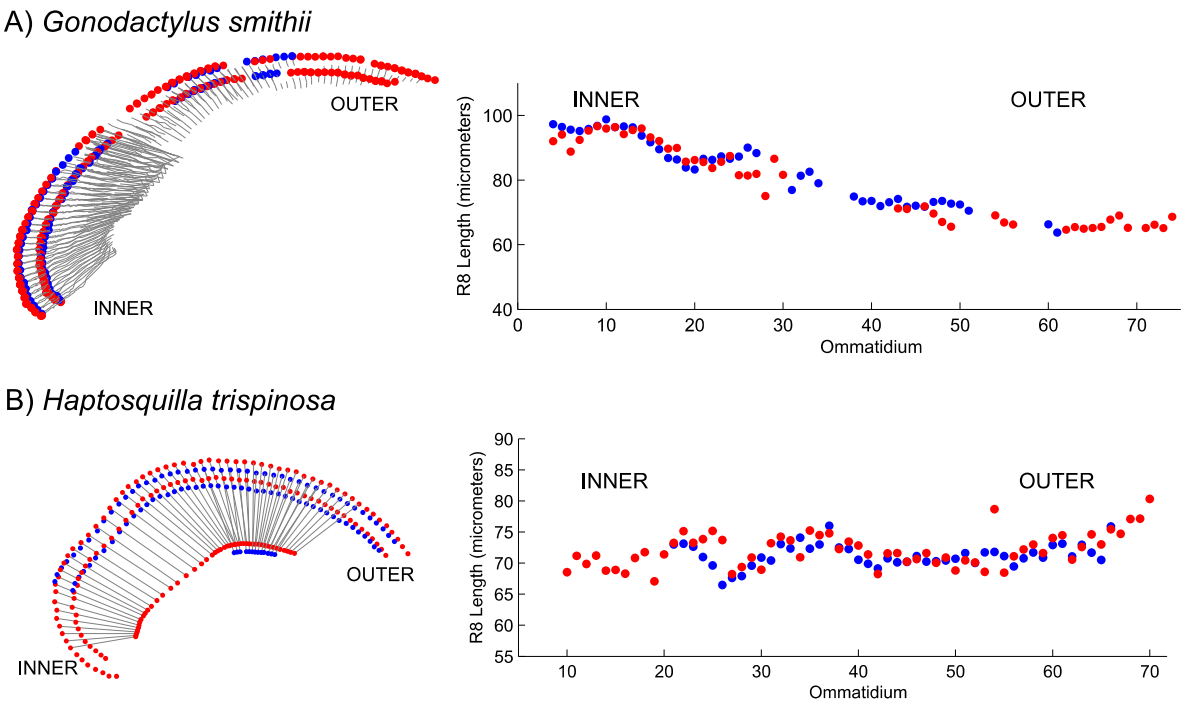

Figure 6: R8 length across entire midband. Reconstruction of the proximal and distal positions of R8 cells from row 5 (blue) and 6 (red) across the length of the midband (from the inner to the outer part of the eye) in *G. smithii* (A) and *H. trispinosa* (B). Left: 3d reconstruction of distal and proximal positions of the R8 cell (and, in some cases, the main rhabdom). Right: R8 length of each ommatidial unit across the whole midband.

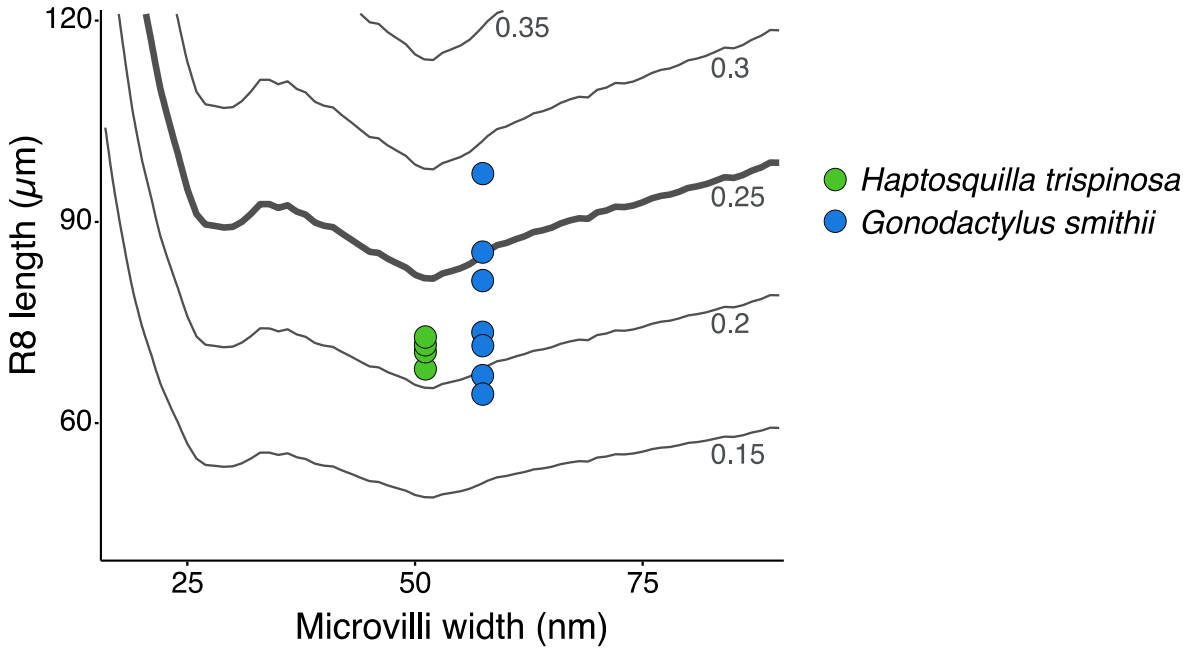

Figure 7: Birefringent properties modelled across whole midband of *H. trispinosa* and *G. smithii*. R8 length obtained from measurements across the whole midband of *H. trispinosa* and *G. smithii* were coupled with the average microvilli width for each species. 7 points are plotted for each species. The consistency in the size of R8 cells in *H. trispinosa* result in many points lying on top on one another. In contrast to this the R8 cells of *G. smithii* vary greatly in function across the midband, altering their birefringent ability and consequently their ability to function as quater wave retarders.

				Row 5				Row 6			
				R1-7		R8		R1-7		R8	
Species	Size mm	Sex	Total Rhabdom µm	Length µm (st dev, n)	% total	Length µm (st dev, n)	% total	Length µm (st dev, n)	% total	Length µm (st dev, n)	% total
Gonodactylus smithii	19	female	375.34	291.3 (3.91, 4)	76.77	88.17 (3.69, 4)	23.23	286.75 (14.68, 6)	77.25	84.47 (4.11, 6)	22.75
	21	male	322.63	244.61 (12.71, 5)	75.82	78.02 (4.12, 5)	24.18				
	55	female	528.21	438.76 (8.58, 5)	83.07	89.45 (3.07, 5)	16.93				
	56	female	418.05	339.22 (22.22, 6)	79.63	86.76 (2.55, 6)	20.37	322.69 (2.14, 6)	78.68	87.43 (4.45, 6)	21.32
	58	male	510.69	454.66 (14.45, 5)	83.27	91.36 (4.95, 5)	16.73	384.83 (35.08, 4)	80.95	90.54 (6.43, 4)	19.05
Haptosquilla trispinosa	16	male	263.37	180.79 (4.44, 6)	70.82	74.5 (2.70, 6)	29.18	199.18 (8.76, 6)	73.37	72.28 (2.55, 6)	26.63
	25	male	269.98	203.07 (5.61, 6)	73.54	73.06 (2.07, 6)	26.46	191.73 (23.62, 6)	72.67	72.1 (2.97, 6)	27.33
	28	male	256.21	179.02 (8.37, 5)	69.81	77.42 (1.00, 5)	30.19	181.11 (6.42, 6)	70.75	74.87 (1.66, 6)	29.25
Lysiosquillina maculata	32	female	288.37	236.88 (8.48, 5)	78.76	63.9 (7.71, 5)	21.24	203.12 (14.25,5)	73.61	72.84 (3.74, 5)	26.39
	72	female	364.07	270.1 (8.33, 6)	75.75	86.46 (3.20, 6)	24.25	281.55 (14.18, 4)	75.77	90.03 (4.02, 4)	24.23
	134	female	438.34	351.89 (11.56, 3)	80.28	86.45 (2.70, 3)	19.72				
Odontodactylus latirostris	37	female	354.14	261.97 (39.25, 6)	73.54	94.25 (4.32, 6)	26.46	260.91 (17.90, 5)	74.11	91.15 (2.62, 5)	25.89
	44	female	373.13	306.06 (2.36, 5)	79.18	80.48 (3.49, 5)	20.82	273.07 (5.28, 5)	75.91	86.65 (4.37, 5)	24.09
	61	female	418.32	332.29 (2.50, 6)	77.81	94.76 (1.63, 6)	22.19	317.43 (5.27, 5)	77.5	92.16 (2.85, 5)	22.5
Odontodacyllus scyllarus	138	female	389.1	303.1 (1.57, 6)	76.91	91 (2.27, 6)	23.09	290.13 (5.09, 6)	75.54	93.96 (1.47, 6)	24.46
	167	male	451.3	365.28 (5.51, 6)	78.54	99.79 (5.82, 6)	21.46	340.52 (10.85, 6)	77.83	97.02 (2.41, 6)	22.17

Table 1: Length measurements for the total rhabdom, R8 and R1-7 rhabdoms. Total rhabdom measurement was achieved by averaging across rows 5 and 6. Average measurements for each individual animal (standard deviation and number of measurements in brackets), including the percentage of total retina occupied by the R8 and R1-7 rhabdom.

			Row 5		Row 6	
			R8 length	Microvilli Width	R8 length	Microvilli Width
Species	**Size mm**	**Sex**	**μm (st dev, n)**	**nm (st dev, n)**	**μm (st dev, n)**	**nm (st dev, n)**
Gonodactylus smithii	19	female	85.54 (4.18, 6)	59.68 (7.08, 15)	83.94 (3.45, 6)	57.43 (5.72, 14)
	55	female	86.60 (3.04, 5)	57.42 (5.85, 18)	87.17 (6.08,3)	60.72 (7.01, 38)
	49	female	87.23 (3.48, 14)	57.71 (7.53, 26)		
	58	male	88.51 (2.02, 12)	52.11 (4.20, 16)	91.14 (4.14, 6)	58.96 (4.31, 23)
	56	female	82.63 (2.04, 15)	51.65 (5.71, 25)	83.47 (1.57, 12)	52.70 (4.05, 26)
	21	male	78.02 (4.12, 5)	54.56 (5.87, 25)		
	68	male	77.51 (2.80, 12)	54.14 (4.08, 17)	75.25 (3.49, 7)	61.39 (4.20, 17)
Gonodactylaceus falcatus	38	male	74.75 (3.41, 15)	46.40 (5.40, 34)	63.42 (3.17, 4)	48.86 (4.89, 17)
	23	male	79.84 (2.52, 6)	45.28 (4.10, 35)	81.36 1.15, 5)	55.5 (5.64, 27)
	44	male	80.37 (3.39, 10)	45.62 (2.09, 20)	79.78 (1.98, 5)	59.76 (5.27, 14)
Odontodacyllus syllarus	45	male	41.87 (2.29, 4)	44.66 (3.45, 8)		
	138	female	91.35 (4.74, 11)	56.38 (7.15, 32)	89.24 (7.67, 6)	59.01 (8.34, 44)
	167	male	95.54 (3.73, 12)	56.31 (7.02, 25)	92.31 (3.01, 16)	74.59 (7.25, 25)
Odontodactylus latirostris	61	female	92.11 (1.70, 10)	64.75 (5.78, 34)	92.93 (2.20, 4)	63.78 (7.32, 32)
	44	female	78.15 (2.53, 7)	61.71 (7.45, 45)	86.06 (3.62, 5)	69.95 (8.36, 37)
	37	female	97.97 (3.65, 18)	71.33 (8.18, 24)	90.22 (3.10, 4)	63.38 (5.52, 28)
Lysiosquillina maculata	134	female	82.23 (3.27, 5)	56.95 (9.26, 18)	81.15 (1.58, 4)	81.47 (10.33, 14)
	72	female	84.60 (4.62, 6)	54.11 (7.23, 19)	84.11 (3.37, 4)	58.19 (6.78, 20)
	32	female	64.03 (7.98, 5)	56.09 (3.58, 15)	65.70 (3.90, 9)	73.05 (10.61, 15)
	200	male	85.8 (4.33, 2)	59.84 (3.12, 25)	79.67 (N/A, 1)	56.53 (3.40, 25)
Haptosquilla trispinosa	16	male	72.21 (5.38, 19)	57.22 (5.75, 31)	66.49 (4.83, 10)	59.76 (6.56, 34)
	16	male	68.88 (1.65, 12)	56.59 (5.19, 41)	68.21 (4.22, 5)	61.08 (7.93, 28)
	25	male	73.31 (2.64, 11)	55.16 (7.29, 25)	71.37 (1.89, 15)	55.98 (6.84, 31)

28	male	65.73 (13.78, 11)	47.37 (3.45, 25)	74.07 (3.63, 13)	58.95 (7.22, 33)
21	female			63.61 (4.74, 7)	48.04 (4.71, 30)

Table 2: Summary of the R8 measurements obtained from each animal. Average length of the R8 and width of the microvilli for both row 5 and 6 with the standard deviation and the number of measurements obtained in brackets (st dev, n) for each animal.